Defining Sudden Stratospheric Warmings in Models: Accounting for Biases in Model Climatologies

Junsu Kim[1+, 2], Seok-Woo Son[2]*, Edwin P. Gerber[3], and Hyo-Seok Park[4]

[1]Numerical Model Research Bureau, Numerical Model Development Division, Seoul, South Korea

[2]School of Earth and Environmental Sciences, Seoul National University, Seoul, South Korea

[3]Courant Institute of Mathematical Sciences, New York University, New York, NY, U.S.A.

[4]Korea Institute of Geoscience and Mineral Resources, Daejeon, South Korea

December, 15, 2016

+ Current affiliation:
Numerical Model Research Bureau, Numerical Model Development Division, Seoul, South Korea

* Corresponding author: Seok-Woo Son, School of Earth and Environmental Sciences, Seoul National University, 1 Gwanak-ro, Gwanak-gu, Seoul, 151-742, South Korea

Abstract

A sudden stratospheric warming (SSW) is often defined as zonal-mean zonal wind reversal at 10 hPa and 60°N. This simple definition has been applied not only to the reanalysis data but also to climate model output. In the present study, it is shown that the application of this definition to models can be significantly influenced by model mean biases; i.e., more frequent SSWs appear to occur in models with a weaker climatological polar vortex. In order to overcome this deficiency, a tendency-based definition, is proposed and applied to the multi-model data sets archived for the Coupled Model Intercomparison Projection phase 5 (CMIP5). In this definition, SSW-like events are defined by sufficiently strong vortex deceleration. This approach removes a linear relationship between SSW frequency and intensity of climatological polar vortex in the CMIP5 models. Models' SSW frequency instead becomes correlated with the climatological upward wave flux at 100 hPa. Lower stratospheric wave activity and downward propagation of stratospheric anomalies to the troposphere are also reasonably well captured. However, in both definitions, the high-top models generally exhibit more frequent SSWs than the low-top models. Moreover, a hint of more frequent SSWs in a warm climate is commonly found.

1. Introduction

A sudden stratospheric warming (SSW) is an abrupt warming event in the polar stratosphere. It occurs mostly in mid and late winters (January and February) and almost exclusively in the Northern Hemisphere (Charlton and Polvani 2007). During this event, the polar stratospheric temperature increases by several tens of degrees within a few days and eventually becomes warmer than mid-latitude temperature. At the same time, the prevailing westerly wind rapidly decelerates and becomes easterly (Quiroz 1975; Labitzke 1977; Andrews et al. 1987). Based on these observations, a SSW has been often defined as a zonal-mean zonal wind reversal in the polar stratosphere associated with a reversal of meridional temperature gradient. In this definition, the so-called WMO definition, temperature gradient criterion affects a very small number of SSWs (Butler et al., 2015). As such, recent studies have often used wind-only definition by ignoring temperature gradient change. This simple definition, which is referred to as the wind-reversal definition in the present study, identifies the onset of SSW as the time at which the 10-hPa zonal-mean zonal wind at 60°N changes its direction from westerly to easterly during the winter (e.g., Charlton and Polvani 2007).

It is important to note that the wind-reversal (or WMO) definition is not the only definition of SSW. As summarized in Palmeiro et al. (2015) and Butler et al. (2015), many definitions for SSWs appear in the literature. These include an area-integrated zonal wind reversal, a tendency-based definition, a Northern Annular Mode (NAM)-based definition, an Empirical Orthogonal Function (EOF)-based definition, and a two-dimensional vortex moment analysis. Palmeiro et al. (2015) documented that the observed frequency of SSW is not highly sensitive to the details of the definitions, although interannual to decadal variability of SSW is somewhat sensitive (particularly the drought of SSWs in the 1990s, cf. Butler et al., 2015). This indicates that long-term statistics of SSWs are not highly sensitive to the definition of SSW. However, this is not necessarily true for climate models in which the climatology and temporal variability differ from observations. Palmeiro et al. (2015) reported that the strength of downward coupling between the stratosphere and the troposphere is sensitive to the SSW definitions and the separation of major and minor warmings: the definition which detects more minor warmings leads to a weaker coupling.

Although application of the wind reversal definition to the climate model output is straightforward, interpretation of the results is not necessarily obvious. For example, SSWs may occur more frequently in the model in which polar vortex variability is anomalously large. However it could also occur in the model if the model's climatological polar vortex is anomalously weak. In the latter case, relatively weak deceleration (i.e. weak wave driving) can result in wind reversal. As an example, Fig. 1 shows zonal-mean zonal wind at 10 hPa and 60°N during winter 1994–1995 from the reanalysis data and during winter 1953-1954 from the Coupled Model Intercomparison Project phase 5 (CMIP5) model. The reanalysis data show rapid deceleration of the zonal wind from mid-January to early February (Fig. 1a). However, the westerly does not shift to an easterly, and according to the WMO definition, this case is defined as a minor warming event rather than SSW. In the model, the polar vortex is significantly weaker than observation (Fig. 1b). Under this weak background wind, relatively weak temporal variability can easily lead to wind reversal. Thus, the model exhibits three SSWs between November and March, although the deceleration of the polar vortex is not as pronounced as the minor warming event in the reanalysis data (Fig. 1a). It is thus not obvious how a model is biased if it does not capture the correct frequency of SSWs, and worse, a model could potentially get the correct frequency with a combination of a weak vortex and strong variability, or vice versa.

[Fig. 1 about here]

This result motivated us to explore the sensitivity of SSW to the model mean bias. For multi-model analysis, previous studies have typically used a WMO-like definition (Charlton et al. 2007; Butchart et al. 2011; Charlton-Perez et al. 2008, 2013). Because SSW frequency in the model can be influenced by the model mean bias as described above, it is questionable whether the quantitative assessment of SSW frequency in the literature is robust. Although not explored in detail, Butchart et al. (2011) did in fact attribute a large intermodel spread in SSW frequency in their multi-model analysis to the different intensities of the polar vortex.

By considering model mean bias, this work revisits the stratospheric variability and SSW frequency in the state-of-the-art climate models archived for the CMIP5. Following previous studies (e.g., Charlton-Perez et al. 2013; Manzini et al. 2014), the models are roughly characterized by grouping them into high-top and low-top models. The low-top models, which have a comparatively poor representation of stratospheric processes, typically underestimate the stratospheric variability and SSW frequency (Charlton-Perez et al. 2013). In this study, it is shown that low-top models underestimate SSW frequency even if a different SSW definition is applied. However, the difference in SSW frequency between the high-top and low-top models becomes smaller when the model mean bias is considered.

This paper is organized as follows. In sections 2 and 3, the data used in this study and the definition of SSW are described. Section 4 explores the climatology, interannual variability, and SSW frequency in the climate change scenario integrations. In section 5, the results are briefly compared with scenario integrations in order to examine the potential changes in SSW frequency in a warmer climate.

2. Data

The daily-mean zonal-mean zonal wind and geopotential height fields were obtained from the 40-year European Centre for Medium-Range Weather Forecasts (ECMWF) Re-Analysis (ERA40; Uppala et al. 2005) for 45 winters of 1957–2002. The results are compared with the climate models archived for CMIP5 models listed in Table 1 for the same period to the reanalysis. All models that provide both the historical and Representative Concentration Pathway 8.5 (RCP8.5) simulations are used. Most analyses are performed for the historical runs. The RCP8.5 runs are examined only in section 5 to evaluate possible changes in SSW frequency in a warm climate. The analysis period of RCP8.5 runs is set to 45 winters from 2044 to 2099 to be compared with 45 winters of historical runs. When multiple ensemble members are available, only the first ensemble member (r1i1p1) is used. An exception is CCSM4, for which the sixth ensemble member (r6i1p1) is used owing to incomplete data in the first ensemble member.

To highlight the model mean bias in the stratosphere, the CMIP5 models are grouped into two subgroups by considering the model top (Charlton-Perez et al. 2013; Manzini et al. 2014). Specifically, models with tops of 1 hPa or higher are classified as high-top models; those with model tops below 1 hPa are classified as low-top models. As described in Table 1, CanESM2 has a model top near 0.5 hPa. It is ambiguous to place this model into either the high-top or low-top category. Following Manzini et al. (2014), this model was therefore classified as a mid-top model.

[Table 1 about here]

It is well documented that after an SSW, stratospheric anomalies tend to propagate downward to the troposphere and the surface (Kodera et al. 2000; Baldwin and Dunkerton 1999). Such downward coupling is often evaluated with a so-called “dripping paint” composite of the NAM index (Baldwin and Dunkerton 2001). In this study, rather than using the EOF-based NAM index, a simple NAM index is used. The NAM index is computed by integrating the geopotential height anomalies from 60°N to the pole at each pressure level (Thompson and Wallace 2000; Gerber et al. 2010). The sign is then flipped to obtain a consistent sign convention of the EOF-based NAM index. The resulting time series are then normalized by one standard deviation of the NAM index of ERA40. This ensures that one-standard-deviation variability in the model is the same as that in the reanalysis data.

3. Definition of SSW

In this study, two definitions of SSW are adopted. The wind-reversal definition, requiring a zonal-mean zonal wind reversal at 10 hPa and 60°N, is used as a reference. When SSW is detected, no subsequent event is allowed within a 20-day interval from the start of the event to avoid a double counting of essentially the same event. The 20-day period is determined in consideration of the thermal damping time scale at 10 hPa. Focusing on mid-winter SSWs, final warming events are excluded by adopting the method proposed by Charlton and Polvani (2007).

As discussed earlier, the wind-reversal definition can be impacted by model mean bias. To reduce such dependency, a new definition, that is based on the zonal-mean zonal wind tendency, (e.g., Nakagawa and Yamazaki 2006; Martineau and Son 2013) is also applied. Specifically, an SSW-like event is identified when the tendency of zonal-mean zonal wind at 10 hPa and 60°N exceeds -1.1 m s^{-1} day^{-1} over 30 days (i.e., polar vortex deceleration of -33 m s^{-1} over 30 days). Here, tendency is computed from 15 days before to after a given day. Note that the reference latitude and pressure level are identical to those used in the wind-reversal definition for a direct comparison.

In a tendency-based definition, the two free parameters, i.e., the threshold value of deceleration (-1.1 m s^{-1} day^{-1}) and the time window for tendency evaluation (30 days), are determined by referring to the observed SSW. The latter, a 30-day window, is inspired by the correlation analysis of Polvani and Waugh (2004). Polvani and Waugh (2004) showed that the upward wave activity entering the stratosphere, integrated over 20 days or longer, leads to a marked weakening of the polar vortex. As discussed in section 4, wave activity associated with SSW is often maintained for about 30 days; thus, a 30-day window is selected in this study. As subsequently described, a slight adjustment of the analysis window (e.g., 20 or 40 days) does not change the overall results.

The minimum deceleration threshold, -1.1 m s^{-1} day^{-1}, is somewhat arbitrary. In this study, this threshold value is selected simply to reproduce the observed SSW frequency. It is known that SSW frequency in the reanalysis data, evaluated at 10 hPa using various definitions, is about 6.4 events per decade (Butler et al. 2015; Palmeiro et al. 2015). The sensitivity of SSW frequency to the threshold value is also discussed subsequently.

It is important to note that the tendency-based definition does not consider a zonal-mean zonal wind reversal. The detected SSW therefore includes major SSW as well as minor warming events in terms of the WMO definition. As such, number of SSWs and their dynamical evolution in the two definitions are not necessarily the same. Table 2 presents the onset dates of SSWs identified by the wind-reversal and tendency definitions in ERA40 (see left column for 60°N cases). Only 18 events are common in the two definitions. A major difference appears in early 1990s. Although no SSWs are identified from 1990 to 1997 in the wind-reversal definition, five SSWs are detected in the tendency definition. Overall, the tendency-based SSWs are more evenly distributed in time. This even distribution, with no significant decadal variability, is similar to NAM-based SSW, as shown in Fig. 2 of Butler et al. (2015).

4. Historical runs

a. Climatology and interannual variability of the polar vortex

Figure 2a shows a vertical cross-section of zonal-mean zonal wind during the Northern Hemisphere winter (December–January–February, DJF) from ERA40. Westerly jets during the boreal winter consist of a tropospheric jet around 30°N and a stratospheric polar vortex around 65°N (Fig. 2a). This structure is well captured by the multi-model mean (MMM) of the high-top models (Fig. 2d). The high-top MMM biases are less than 2 m s^{-1} (shaded), which is not significantly different from the ERA40 data over most regions. In contrast, the low-top MMM show a stronger polar vortex than that in the reanalysis data (Fig. 2g). Their mean biases are larger than 5 m s^{-1} at 10 hPa and 40°N, indicating that the polar vortex in the low-top models is biased equatorward. Although a causal relationship is unclear, the wind biases shown in Fig. 2g could partly reflect a lack of SSWs in the low-top models, as compared with reanalyses and the high-top models (Charlton-Perez et al. 2013).

[Fig. 2 about here]

The low-top models also exhibit significantly larger biases in their interannual variability in the extratropical stratosphere than the high-top models (compare Fig. 2e and h). This result, which agrees well with the findings of Charlton-Perez et al. (2013), is to some extent anticipated because the low-top models do not resolve realistic stratospheric processes. It is interesting to note that both high-top and low-top models underestimated tropical stratospheric variability. This arises from the lack of quasi-biennial oscillation (QBO) in most models (e.g. Kim et al. 2013). Because the QBO can influence the Northern Hemisphere wintertime stratospheric polar vortex (Holton and Tan 1980; Garfinkel et al. 2012), the lack of QBO activity in the models could adversely affect extratropical stratospheric variability on interannual time scales.

b. Intraseasonal variability of the polar vortex

The low-top models again show larger biases in intraseasonal variability of polar vortex, quantified by daily one standard deviation, than the high-top models (Figs. 2f, i). Here, before computing daily variability, seasonal-mean value in each winter is subtracted from daily anomalies to remove the interannual variability. These biases in intraseasonal variability are not confined within the stratosphere but extend to the troposphere in high latitudes as well. This could indicate that the poorly-represented stratospheric process in the low-top models may introduce bias in the upper troposphere.

The relationship between the deseasonalized daily zonal-mean zonal wind variability and climatological zonal-mean zonal wind at 10 hPa and 60°N is further illustrated in Fig. 3, where the high-top and low-top models are reasonably well separated into the two clusters. The daily variability in the high-top models is about 12 m s^{-1} which is close to the observation of about 13 m s^{-1}, while that in the low-top models is only about 8 m s^{-1}. This may indicate less frequent SSWs in the low-top models. In addition, the intermodel spread among the low-top models is larger than that among the high-top models in both climatology and intraseasonal variability. This result confirms that a high model top is helpful for reproducing the stratospheric mean state and temporal variability (Charlton-Perez et al. 2013; Manzini et al. 2014).

[Fig. 3 about here]

c. SSW statistics

Extending the results of Charlton-Perez et al. (2013), the SSW frequency of ERA40 was first evaluated by using the wind reversal definition (Fig. 4a). The long-term mean SSW frequency is about 6.4 events per decade, as shown by the horizontal line in the figure. CMIP5 models typically underestimate this frequency (Charlton-Perez et al. 2013). The SSW frequency in the high-top models varies from 3 to 9 events per decade (red bars), with a MMM frequency of 5.8 events per decade (rightmost red bar). This MMM frequency is reasonably close to the reference frequency. In contrast, the low-top models exhibit only up to 4 events per decade (blue bars in the figure), with 1.8 events per decade on average (rightmost blue bar). More importantly, the intermodel spread in the two groups of models does not overlap, indicating that the low-top models are well separated from the high-top models in terms of SSW frequency (see also Fig. 3. This result supports the findings of Charlton-Perez et al. (2013), who analyzed a smaller numbers of CMIP5 models. Somewhat surprisingly, the mid-top model, CanESM2, shows significantly high SSW frequency than any other models, with 10.7 events per decade. Such high frequency is associated with a weak background wind in this model, as illustrated in Figs. 1b and 3.

[Fig. 4 about here]

The SSW frequency is also evaluated using the tendency-based definition (Fig. 4b). By construction, SSW frequency in this definition remains 6.4 events per decade in ERA40. Although each model shows SSW frequency that differs from the wind-reversal definition, its frequency for the high-top MMM is 6.2 events per decade, which is quantitatively similar to the observed frequency. Within the uncertainty range, this frequency is also similar to that derived from the wind-reversal definition: the SSW frequency in the WMO definition is 5.8 events per decade (Fig. 4a), whereas the tendency-based definition illustrates 6.2 events per decades (Fig. 4b). The intermodel spread, however, is only half of that of the wind-reversal definition (compare Figs. 5a and b). This result clearly suggests that the tendency definition is less sensitive to intermodel differences (i.e., model mean biases) as the wind-reversal definition.

The low-top models again show fewer SSWs than the high-top models, with a MMM frequency of 3.7 events per decade. This indicates that regardless of the definition, the low-top models tend to underestimate the observed SSW frequency. Here, it is important to note that the resulting SSW frequency is larger than that derived from the wind-reversal definition in Fig. 4a, (i.e., 3.7 versus 1.8 events per decade). In other words, the difference in SSW frequency between the high-top and low-top models becomes smaller when the tendency definition is used. In fact, the intermodel spread of SSW frequency in the low-top models now overlaps that in the high-top models (Fig. 4b). This result indicates that the frequency of extreme stratospheric event may be less sensitive to the model top than that previously reported (e.g., Charlton-Perez et al. 2013). This is particularly true if the two models with extremely rare SSWs (i.e., CSIRO-Mk3-6-0 and INMCM4) are excluded from the low-top MMM.

The only mid-top model, CanESM2, shows a significant reduction in SSW frequency from the wind reversal definition to the tendency definition, as indicated by the green bars in Figs. 4a and b. When the tendency definition is used, SSW frequency becomes close to the observed frequency. The CanEMS2, which is a clear outlier in terms of the wind-reversal SSWs not belonging to either high-top or low-top models, is not an outlier any more.

The above results are all based on intercomparison of high-top and low-top models. However, even in each group, individual models are very different in many aspects such as dynamic core, physics, resolution, and ocean models; therefore, direct comparison of these models may not be straightforward. In this regard, comparison of two different experiments from the same modeling institutes might be insightful. As indicated in Table 1, the Centro Euro-Mediterraneo sui Cambiamenti Climatici (CMCC) provides two experiments, i.e., CMCC-CM and CMCC-CMS. The former is a low-top version, whereas the latter is a high-top version of the model. Figure 4b shows that CMCC-CMS simulates realistic SSW frequency and significantly more frequent SSW than CMCC-CM, which is consistent with MMM comparison. A pair of experiments from Institut Pierre Simon Laplace Climate model 5A (IPSL-CM5A), i.e., IPSL-CM5A-low resolution (LR) and IPSL-CM5A-medium resolution (MR) differing in horizontal resolution, further shows that the model with a higher horizontal resolution (IPSL-CM5A-MR) has more frequent SSW than IPSL-CM5A-LR. However, MPI-ESM-LR and MPI-ESM-MR, which have different vertical resolutions but the same model top, show a similar SSW frequency. A comparison of the Model for Interdisciplinary Research on Climate-Earth System Model (MIROC-ESM) and that coupled with stratospheric chemistry (MIROC-ESM-CHEM) also shows no significant difference. All together, these results may suggest that SSW frequency is more sensitive to the model top and horizontal resolution than to vertical resolution and interactive chemistry (Scott et al. 2004). However, to confirm this speculation, additional modeling studies with systematic varying of model configurations are needed.

To highlight the dependency of SSW frequency to the model mean bias, Fig. 5a illustrates the relationship between DJF-mean zonal-mean zonal wind at 10 hPa and 60°N and SSW frequency derived from the wind-reversal definition. The high-top, mid-top, and low-top models are indicated in red, green, and blue, respectively, whereas ERA40 is shown by a black dot. A strong negative correlation is evident with a correlation coefficient of -0.63, which is statistically significant at the 95% confidence level. This clearly indicates that SSW occurs less frequently as the background wind becomes stronger (or, alternatively, fewer SSW leads to a stronger vortex). Such negative correlation is somewhat weak in the low-top models owing to a few outliers that have almost no SSWs. Without these outliers (i.e., CSIRO-MK3-6-0 and MIROC5), the negative correlation becomes statistically significant.

[Fig. 5 about here]

Figure 5a also shows that the high-top models are well separated from the low-top models. Except for two models, most low-top models show a stronger polar vortex than ERA40. This strong polar vortex does not allow a wind reversal unless stratospheric wave driving is sufficiently strong (or may inhibit the resonant vortex splitting mechanism; Esler and Scott 2005). This result confirms that the difference between the high-top and low-top models shown in Fig. 4a is caused partly by the model mean biases. Another factor that may explain the less frequent SSW in the low-top models is relative weak wave driving. As shown in Fig. 5c, the low-top models exhibit somewhat weaker wave activity than the high-top models. Here, wave activity is quantified by integrating the zonal-mean eddy heat flux at 100 hPa over 45–75°N (Polvani and Waugh 2004).

The right-hand panels of Fig. 5 are identical to those on the left except for the tendency definition. The linear relationship evident in Fig. 5a essentially disappears in Fig. 5b. also shows that the high-top models are well separated from the low-top models. Except for two models, most low-top models show a stronger polar vortex than ERA40. This strong polar vortex does not allow a wind reversal unless stratospheric wave driving is sufficiently strong (or may inhibit the resonant vortex splitting mechanism (Fig. 5d) such that more frequent SSW occurs when the wave activity in the lower stratosphere is stronger. This result may indicate that the tendency definition is more dynamically constrained than the wind-reversal definition. Here, note that most models underestimate wave activity in the lower stratosphere. This is consistent with the fact that most models underestimate the SSW frequency regardless of the model top (Fig. 4b).

The relationship among the SSW frequency, daily zonal-mean zonal wind variability, and DJF-mean zonal-mean zonal wind at 10 hPa and 60°N is summarized in Fig. 6, which combines the essential results of Figs. 3, 5a, and 5b. The CMIP5 models generally have realistic time-mean polar vortices but too little variability (e.g., climatology of 25–35 m s^{-1} in Fig. 6). For both the wind-reversal and tendency definitions, the CMIP5 models exhibit less frequent SSWs with a weaker intraseasonal variability in comparison to ERA40. This is particularly true for the low-top models. However, unlike the tendency-based SSW frequency, the wind-reversal SSW frequency shows a strong dependency to the climatological wind with a less frequent SSW for strong background wind (smaller circles for climatological wind stronger than 35 m s^{-1}). This impact of model mean bias is effectively removed in the tendency-based SSW definition.

[Fig. 6 about here]

We next explore the sensitivity of sub-seasonal distribution of SSW frequency to the SSW definition. Previous studies have reported that climate models have trouble producing the correct monthly distribution of SSW frequency under the wind reversal definition (Schmidt et al. 2013; Charlton and Polvani 2007). Fig. 7 shows the monthly distribution of SSWs for the wind reversal and wind tendency definitions; SSWs from ERA40 reanalysis are shown in black, and those from high-top and low-top models are shown with red and blue, respectively. With the wind reversal definition (Fig. 7a), SSWs in ERA40 occur throughout the extended winter season, but peak in mid winter (January). As noted by earlier studies, the distribution of reversal events is too evenly spread across the extended winter in high top models, and heavily biased towards late winter in low top models.

[Fig. 7 about here]

In ERA40, the wind tendency definition tends to concentrate SSWs in January and February (Fig. 7b). We believe that this stems from the fact that a large absolute deceleration of the vortex in part depends upon a strong initial vortex. (Once the winds reverse, Rossby wave propagation is inhibited, limiting any further wave breaking which would be needed to drive the winds more strongly negative.) Hence events are favored by the strong climatological wind in mid-winter, and final warmings are naturally excluded under this definition, given the weakness of the vortex in late winter. This focusing of events in the mid winter is captured in high-top models, although the distribution is still too flat, with too many events in November, December, and March and too few in January and February. Low top models fail to capture the effect, and events are still concentrated at the very end of winter. We suspect this delay is associated with the delayed breakup of the vortex: variability in the low top models appears more like that of the observed Southern Hemisphere than the observed Northern Hemisphere.

d. SSW dynamics

The SSWs identified by the two definitions can have different dynamical evolution. For example, linear wave dynamics suggest that vertical propagation of planetary-scale waves, which drive SSW, can be restricted if the zonal wind in the stratosphere becomes easterly. However, this may not be the case in the tendency-based SSW because a wind reversal to easterly is not guaranteed, and minor warming events (in term of the WMO definition) are included. To address this issue, we investigated the wave activity over the course of an SSW. Figure 8 presents a composite of the temporal evolution of a zonal-mean eddy heat flux at 100 hPa integrated over 45–75°N for the two SSW definitions. The heat flux increases before the onset of an SSW, then rapidly decreases afterward. Although the evolution of wave activity is qualitatively similar in the two definitions, the tendency-based definition showed a somewhat slower decay, as shown by the black lines in Fig. 8. In this respect, the tendency events are less "sudden". Furthermore, small amount of planetary-scale waves still propagates into the stratosphere even after the event onset because not all events accompany a wind reversal.

[Fig. 8 about here]

The wind-reversal SSWs are associated with slightly stronger and more concentrated wave forcing than that the tendency-based SSWs. However, the time-integrated wave activity over 30 days before the onset of SSW is comparable in the two definitions, indicating similar net wave driving. Figure 8 also shows that the wave activity in the high-top models is somewhat stronger than that in the low-top models from lag −20 to 0 days. Consistent with this result, the intensity of SSWs in terms of zonal wind deceleration is somewhat stronger in the high-top models than that in the low-top models (not shown). This result suggests that improved vertical resolution and higher model top is helpful in simulating more realistic SSWs.

As discussed previously, SSWs have received much attention in recent decades because of its influence on tropospheric circulation and surface climate (Baldwin and Dunkerton 2001). By comparing a subset of CMIP5 models, Charlton-Perez et al. (2013) reported that high-top models tend to have more persistent anomalies than low-top models in the troposphere. In Fig. 9, a similar comparison is made in terms of NAM-index anomalies for the two SSW definitions. For ERA40, the tendency-based SSW exhibits a stronger phase change than the wind-reversal SSW in NAM anomalies in both the lower stratosphere and the troposphere (Figs. 9a, b), but an overall weaker (less negative) tropospheric NAM response following the event. Such a difference is also evident in analysis of individual models. This result implies that the wind-reversal SSWs are somewhat deeper than the tendency-based SSWs. Although the exact reason is not clear, it is consistent with stronger and more abrupt wave flux changes in the wind-reversal events (Fig. 8). A rather weak SSW in the tendency definition may result from the inclusion of minor warmings (in terms of WMO definition) and the spread of the onset dates. In the tendency definition, zonal-wind tendency is computed with a 30-day time window and the central day is chosen as the onset day. This central day is not necessarily the day of maximum vortex deceleration. This mismatch could cause weaker SSWs and weaker downward coupling.

However, the resulting downward coupling is still within an uncertainty range of various SSW definitions as shown in Palmeiro et al. (2015; see their Fig. 6).[Fig. 9 about here]

It is important to note from Fig. 9 that SSW-induced NAM-index anomalies in the lower stratosphere tend to persist longer in the high-top models than those in the low-top models. Similarly, the tropospheric anomalies are stronger and persisted slightly longer in the high-top models than in the low-top models in the two definitions. This result suggests that the timescale of SSW and downward coupling are somewhat sensitive to the model top.

e. sensitivity test

Both the WMO wind only and tendency-based definitions utilize zonal-mean zonal wind at a fixed latitude (60°N) to evaluate the polar vortex weakening. This latitude corresponds to the vortex boundary in the reanalysis data (Butler et al. 2015). However, the same may not be true when using the models. In fact, as shown in Fig. 2, the latitudinal structure of polar vortex in the model differs from that in the reanalysis data, and 60°N is not the vortex boundary in all models. This is particularly true for the low-top models (Fig. 2g). To test this possibility, all analyses were repeated by replacing the fixed reference latitude with the model-dependent reference latitudes. The latitude of the maximum zonal-mean zonal wind at 10 hPa in long-term climatology was chosen for each model, and the SSW frequency was again evaluated. This modification results in an increased SSW frequency of about half an event per decade in both the high-top and low-top models (not shown). However, the overall conclusion of more frequent SSW in high-top models than those in low-top models does not change.

We also tested the sensitivity of the tendency-based SSW to the threshold value of deceleration and the time window for tendency evaluation. The top panel in Fig. 10 presents the

SSW frequency calculated from ERA40 as a reference. As would be expected, the SSW frequency generally increased as the threshold value decreases (i.e., SSW was more frequent for a weaker threshold value). The SSW frequency also decreases with an increase in the time window. Notably, the SSW frequency in the high-top models is comparable to that in ERA40 if the observed SSW frequency of 6–8 events per decade was selected as a reference (near-zero line in Fig. 10c), but would be biased high (low) if stricter (weaker) criteria are applied. The low-top models, however, exhibited a significantly smaller number of SSWs (Fig. 10d) under all conditions. This underestimation is not highly sensitive to the parameters used in the tendency-based SSW definition. Figure 10b further shows the differences in SSW frequency between the high-top and low-top models. In general, the high-top models showed more frequent SSW, which indicates that the SSW frequency difference between the two groups of models is quite robust.

[Fig. 10 about here]

Figure 11 further illustrates the relationship between the SSW frequencies to background wind as in Figs. 5a and 5b but at 65°N and 70°N. Overall results are essentially same to the analysis at 60°N (compare Fig. 5a, 5b, and Fig. 11). A strong negative correlation in the wind-reversal definition (Figs. 11a and 11c) disappears in the tendency definition at both latitudes Figs. 11b, 11d). This result suggests the results presented in the previous section are not sensitive to the choice of reference latitude.

[Fig. 11 about here]

5. SSWS in future climate projections

We now compare the SSW frequency in the recent past with that in the 21st century. Figure 12 illustrates the projected changes in SSW frequency under the RCP8.5 scenario by the end of 21st century. The wind reversal definition suggests slightly more frequent SSW in the warm climate (Fig. 12a), which agrees well with the results of Charlton-Perez et al. (2008). The high-top models generally show a more positive trend in SSW frequency than the low-top models; 8 out of 12 high-top models show an increasing trend (Fig. 12c). However, the low-top models do not show a clear trend if CSIRO-MK3-6-0. If CSIRO-MK3-6-0, which fails to simulate any SSWs, is excluded, the number of the models with an increasing and decreasing trend is even.

[Fig. 12 about here]

McLandress and Shepherd (2009), however, suggested that the above increasing trend of SSW frequency may be partly attributed to changes in background wind rather than those in wave activity. In response to increasing greenhouse gas concentration, the polar vortex tends to weaken (e.g., McLandress and Shepherd 2009; Manzini et al. 2014; Mitchell et al. 2012; Ayarzagüena et al. 2013). If the background wind becomes weaker in a warmer climate, the chances of a wind reversal may increase, resulting in more frequent SSW. Such an increase in SSW frequency, however, is misleading unless the wave forcing systematically changes (McLandress and Shepherd 2009). By using a relative definition which is not sensitive to the mean flow change, McLandress and Shepherd 2009) in fact showed that SSW frequency does not change much in their model.

This idea is evaluated with a tendency definition (Fig. 12b). It is found that, in both the high-top and low-top models, SSW frequency is projected to slightly increase in the future.

Although the absolute change is not statistically significant, 21 of 27 CMIP5 models show an increasing trend (Fig. 12d). Such behavior is also evident upon separate examination of the high-top and low-top models, with 9 of 12 high-top and 11 of 14 low-top models showing increasing trends. This result suggests that stratospheric extreme events may indeed increase in the future climate. To identify the dynamical mechanism(s), further analyses are needed.

6. Summary and discussion

The present study suggests that the wind metric emphasized by the WMO definition of an SSW, i.e., a wind reversal at 10 hPa and 60°N, can be impacted by model mean biases (McLandress and Shepherd 2009). The definition can straightforwardly be applied to models, but the interpretation may be more complicated. If the climatological polar vortex of the model is stronger than observation, it tends to allow less frequent SSWs. Such a relationship is robustly found in the CMIP5 models, regardless of the reference latitude (e.g., 60°N, 65°N, and 70°N), indicating that the previous multi-model studies on wind-reversal SSW are likely influenced by the model mean biases and long-term mean flow changes (Fig. 2).

An alternative definition of extreme vortex variability, aiming to make it independent of model mean biases, is proposed in the present study. This definition detects SSWs by examining the zonal-mean zonal wind tendency at 10 hPa and 60°N. In this definition, the linear relationship between SSW frequency and the intensity of climatological polar vortex, which is evident in the wind-reversal definition, essentially disappears. Final warming events are also naturally filtered out. More importantly, SSW frequency becomes highly correlated with wave activity at 100 hPa. This result indicates that the tendency-based definition is more dynamically constrained than the wind-reversal definition. This is anticipated because the zonal-mean zonal wind tendency is directly related to eddy heat (and momentum flux) divergence in the transformed Eulerian mean framework (e.g., Dunn-Sigouin and Shaw 2015).

The tendency-based definition results in more frequent SSWs than the wind-reversal definition in the climate models, particularly in the low-top models, even though it is constructed to have no effect on the SSW frequency in ERA-40 reanalysis. This indicates that the significant difference in SSW frequency between the low-top and high-top models reported in previous studies (e.g., Charlton-Perez et al. 2013) can be attributed, at least in part, to model mean bias rather than wave driving. However, in both definitions, the high-top models show more realistic SSW statistics than the low-top models. Particularly, the low-top models significantly underestimate SSW frequency, in consistent with relatively weak lower-stratospheric wave activities, and fail to simulate its monthly distribution. This result indicates that a high model top and more accurate stratospheric representation are necessary for simulating realistic SSW. It is also found that in both definitions, the SSW frequency is projected to increase in a warm climate. These results are qualitatively consistent with those in previous studies (e.g., Charlton-Perez et al., 2008, 2013).

The SSWs, detected by the different definitions, may have different dynamical and physical properties (Martineau and Son 2015). In fact, the tendency-based SSWs show quantitatively different temporal evolution from the wind-reversal SSWs. The former is associated with less focused and slightly weaker wave activity than the latter. This difference leads to slightly weaker persistence of stratospheric anomalies and a weaker downward coupling in the tendency-based SSW. However, such differences are still within the uncertainty of various SSW definitions (Palmeiro et al. 2015).

It should be emphasized that development of a new SSW definition is not our primary intent in this study. Our objectives are to re-examine the SSW frequency in CMIP5 models by considering the model mean bias and to test the robustness of previous studies by applying the different SSW definitions. Certainly, other approaches can be used to define stratospheric extreme events that are free from model mean biases as discussed in Palmeiro et al. (2015), Butler et al. (2015), and Martineau and Son (2015). Since many different definitions of SSW have been used in the literature, further discussion on their weaknesses and strengths would be valuable (Butler et al. 2015).

Acknowledgement

The authors thank all of the reviewers for their helpful comments. The authors thank Dr. Gwangyong Choi for offering helpful discussion. This work was funded by the Korea Meteorological Administration Research and Development Program under Grant KMIPA 2015-2094 and the US National Science Foundation, through grant AGS-1546585.

References

Andrews, D. G., J. R. Holton, and C. B. Leovy, 1987: Middle atmosphere dynamics. Academic Press, 489 pp.

Ayarzagüena, B., U. Langematz, S. Meul, S. Oberländer, J. Abalichin, and A. Kubin, 2013: The role of climate change and ozone recovery for the future timing of major stratospheric warmings. Geophys. Res. Lett., 40, 2460-2465.

Baldwin, M. P., and T. J. Dunkerton, 1999: Propagation of the Arctic oscillation from the stratosphere to the troposphere. J. Geophys. Res., 104, 30937-30946.

——, 2001: Stratospheric harbingers of anomalous weather regimes. Science, 244, 581-584.

Butchart, N., and Coauthors, 2011: Multimodel climate and variability of the stratosphere. J. Geophys. Res. Atmos., 116, D05102.

Butler, A. H., D. J. Seidel, S. C. Hardiman, N. Butchart, T. Birner, and A. Match, 2015: Defining sudden stratospheric warmings. Bull. Amer. Meteor. Soc., 96, 1913-1928.

Charlton-Perez, A. J., L. M. Polvani, J. Austin, and F. Li, 2008: The frequency and dynamics of stratospheric sudden warmings in the 21st century. J. Geophys. Res., 113, D16116.

Charlton-Perez, A. J., and Coauthors, 2013: On the lack of stratospheric dynamical variability in low-top versions of the CMIP5 models. J. Geophys. Res., 118, 2494-2505.

Charlton, A. J., and L. M. Polvani, 2007: A new look at stratospheric sudden warmings. Part I: Climatology and modeling benchmarks. J. Climate, 20, 449-469.

Charlton, A. J., and Coauthors, 2007: A new look at stratospheric sudden warmings. Part II: Evaluation of numerical model simulations. J. Climate, 20, 470-488.

Cohen, J., D. Salstein, and K. Saito, 2002: A dynamical framework to understand and predict the major Northern Hemisphere mode. Geophys. Res. Lett., 29, 51.

Dunn-Sigouin, E., and T. A. Shaw, 2015: Comparing and contrasting extreme stratospheric events, including their coupling to the tropospheric circulation. J. Geophys. Res. Atmos., 120, 1374-1390.

Esler, J. G., and R. K. Scott, 2005: Excitation of Transient Rossby Waves on the Stratospheric Polar Vortex and the Barotropic Sudden Warming. J. Atmos. Sci., 62, 3661-3682.

Garfinkel, C. I., T. A. Shaw, D. L. Hartmann, and D. W. Waugh, 2012: Does the Holton–Tan Mechanism Explain How the Quasi-Biennial Oscillation Modulates the Arctic Polar Vortex? J. Atmos. Sci., 69, 1713-1733.

Gerber, E. P., and Coauthors, 2010: Stratosphere-troposphere coupling and annular mode variability in chemistry-climate models. J. Geophys. Res., 115, D00M06.

Holton, J. R., and H.-C. Tan, 1980: The Influence of the Equatorial Quasi-Biennial Oscillation on the Global Circulation at 50 mb. J. Atmos. Sci., 37, 2,220-2208.

Kim, J., K. M. Grise, and S.-W. Son, 2013: Thermal characteristics of the cold-point tropopause region in CMIP5 models. J. Geophys. Res. Atmos., 118, 8827-8841.

Kodera, K., Y. Kuroda, and S. Pawson, 2000: Stratospheric sudden warmings and slowly propagating zonal-mean zonal wind anomalies. J. Geophys. Res. Atmos., 105, 12351-12359.

Labitzke, K., 1977: Interannual Variability of the Winter Stratosphere in the Northern Hemisphere. Mon. Wea. Rev., 105, 762-770.

Manzini, E., and Coauthors, 2014: Northern winter climate change: Assessment of uncertainty in CMIP5 projections related to stratosphere-troposphere coupling. J. Geophys. Res. Atmos., 119, 2013JD021403.

Martineau, P., and S.-W. Son, 2013: Planetary-scale wave activity as a source of varying tropospheric response to stratospheric sudden warming events: A case study. J. Geophys. Res. Atmos., 118, 10,994-911,006.

——, 2015: Onset of circulation anomalies during stratospheric vortex weakening events: the role of planetary-scale waves. J. Climate, 28, 7347-7370.

McLandress, C., and T. G. Shepherd, 2009: Impact of Climate Change on Stratospheric Sudden Warmings as Simulated by the Canadian Middle Atmosphere Model. J. Climate, 22, 5449-5463.

Mitchell, D. M., S. M. Osprey, L. J. Gray, N. Butchart, S. C. Hardiman, A. J. Charlton-Perez, and P. Watson, 2012: The Effect of Climate Change on the Variability of the Northern Hemisphere Stratospheric Polar Vortex. J. Atmos. Sci., 69, 2608-2618.

Nakagawa, K. I., and K. Yamazaki, 2006: What kind of stratospheric sudden warming propagates to the troposphere? Geophys. Res. Lett., 33, L04801.

Palmeiro, F. M., D. Barriopedro, R. Garcia-Herrera, and N. Calvo, 2015: Comparing Sudden Stratospheric Warming Definitions in Reanalysis Data. J. Climate, 28, 6823-6840.

Polvani, L. M., and D. W. Waugh, 2004: Upward wave activity flux as a precursor to extreme stratospheric events and subsequent anomalous surface weather regimes. J. Climate, 17, 3,548-543,554.

Quiroz, R. S., 1975: The Stratospheric Evolution of Sudden Warmings in 1969–74 Determined from Measured infrared Radiation Fields. J. Atmos. Sci., 32, 211-224.

Schmidt, H., and Coauthors, 2013: Response of the middle atmosphere to anthropogenic and natural forcings in the CMIP5 simulations with the Max Planck Institute Earth system model. Journal of Advances in Modeling Earth Systems, 5, 98-116.

Scott, R. K., D. G. Dritschel, L. M. Polvani, and D. W. Waugh, 2004: Enhancement of Rossby Wave Breaking by Steep Potential Vorticity Gradients in the Winter Stratosphere. Journal of the Atmospheric Sciences, 61, 904-918.

Thompson, D. W. J., and J. M. Wallace, 2000: Annular modes in the extratropical circulation. Part I: Month-to-month variability. J. Climate, 13, 1000-1016.

Uppala, S. M., and Coauthors, 2005: The ERA-40 re-analysis. Quart. Jour. Royal. Met. Soc., 612, 2961-3012.

Tables

Table 1 CMIP5 models used in this study and their classification.

Table 2 Sudden stratospheric warming (SSW) identified from the wind reversal and wind tendency definitions.

Figures

Fig. 1 Zonal-mean zonal winds (m s^{-1}) at 10 hPa and 60°N for (a) ERA40 and (b) CanESM2 models. The thin line across the x-axis denotes the 0 m s^{-1} threshold.

Fig. 2 (a) Latitude and height cross-section of the climatological zonal-mean zonal winds ([u]; m s−1) averaged from December to February (DJF) in ERA40. The contour interval is 10 m s−1, and the zero line is indicated with a thick black line. (center and right) Same as (a) but for interannual variability of the DJF-mean [u] (center) and daily variability of [u] in DJF (right). For the daily variability, the mean value for each winter was subtracted from daily anomalies to remove the impact of the interannual variability. (middle and bottom rows) Same as the top row but for high-top (middle) and low-top (bottom) models. Statistically insignificant (t-test; $p > 0.05$) values are hatched, and difference from ERA40 (model-ERA40) is shown by shading.

Fig. 3 Scatter plot of the zonal-mean zonal wind climatology at 10 hPa and at 60°N and its daily standard deviation from CMIP5 models. Red, green, blue, and black colors indicate high-top, mid-top, and low-top models and ERA40 reanalysis, respectively. Solid lines range ±1 standard deviation among models while centered on their multi-model mean.

Fig. 4 Sudden stratospheric warming (SSW) frequency derived from (a) the wind reversal definition and (b) the wind tendency definition. Low-top, mid-top, and high-top models are colored blue, green, and red, respectively. The SSW frequency in ERA40 is indicated by the black horizontal line. Multi-model mean frequency and intermodel spread (1 standard deviation) are shown at the right of each panel.

Fig. 5 (a, b) Scatter plot of climatological zonal-mean zonal wind at 10 hPa and 60°N and sudden stratospheric warming (SSW) frequency for the wind reversal definition (left) and the wind tendency definition (right). (c, d) Same as top panels but for eddy heat flux at 100 hPa integrated over 45–75°N. Low-top, mid-top, and high-top models are colored blue, green, and red, respectively. Black-dotted lines indicate the reference values in ERA40. The numbers shown in each panel denote the correlation coefficients for all (black), high-top (red), and low-top (blue) models. Statistically significant correlation coefficient at the 95% confidence level is indicated by the asterisk.

Fig. 6 Same as Fig. 3 but for sudden stratospheric warming (SSW) frequency introduced using the wind reversal definition (left) and the wind tendency definition (right). The circle size indicates the SSW frequency per decade. Low-top, mid-top, and high-top models are colored blue, green, and red, respectively.

Fig. 7 Distribution of stratospheric warmings by month in ERA40 reanalysis (black), high-top (red), and low-top models (red) derived from (top) the wind reversal definition and (bottom) the wind tendency definition. Vertical lines at high-top and low-top models indicate the ±1 standard deviation of SSW frequency from the mean of each model.

Fig. 8 Multi-model mean time series of zonal-mean eddy heat flux at 100 hPa integrated over 45–75°N during sudden stratospheric warming (SSW) detected by the wind reversal definition (left) and the wind tendency definition (right). Lag zero indicates the onset of SSW. Low-top and high-top models are denoted by blue and red colors, respectively. The reference time series, derived from ERA40, is shown in black.

Fig. 9 Time-height development of the northern annular mode (NAM) index during sudden stratospheric warming (SSW) events, as detected by the wind reversal definition (left) and the wind tendency definition (right) for ERA40 (top), high-top (middle), and low-top (bottom) models. The NAM index is based on polar-cap averaged geopotential height (>60°N). Shading interval of 1.0 is indicated by a white line. Hatching shows insignificant values (95%) when the multi-model spread is considered.

Fig. 10 (a) Sudden stratospheric warming (SSW) frequency as a function of the threshold value of the zonal-mean zonal wind tendency at 10 hPa and 60°N and the evaluated time window for ERA40. (b) Difference between the high-top and low-top models. Difference between ERA40 and (c) high-top and (d) low-top models. Values statistically insignificant at the 95% confidence level are hatched. The two low-top models were ignored because their SSWs are extremely rare. The SSW frequency of six to eight events per decade from ERA40 is shown by with thick black lines in each panel. The numbers at the upper right corner in each panel indicates SSW frequency or its difference from ERA40 when the -1.1 m s-1 day-1 threshold and 30-day time window are used.

Fig. 11 (a, b) Scatter plot of climatological zonal-mean zonal wind at 10 hPa and 65°N, and SSW frequency for (left) the wind reversal definition and (right) the wind tendency definition. (c, d) Same as top panels but for zonal wind at 70°N. Low-top, mid-top, and high-top models are colored with blue, green, and red, respectively. Black-dotted lines indicate the reference values in ERA40. Numbers shown in each panel denote the correlation coefficients for (black) all, (red) high-top, and (blue) low-top models. Statistically significant correlation coefficient at the 95% confidence level is indicated by asterisk.

Fig. 12 (a, b) Same as Fig. 4 but for RCP8.5 runs. (c, d) Difference in sudden stratospheric warming (SSW) frequency between RCP8.5 and historical runs.

Table 1 CMIP5 models used in this study and their classification.

Model Name	Center	Vertical Level	Model Top	Classification
ACCESS1-0	ACCESS	38	39 km	Low
ACCESS1-3	ACCESS	38	39 km	Low
BCC-CSM1-1	BCC	26	2.917 hPa	Low
BCC-CSM1-1-M	BCC	26	2.917 hPa	Low
BNU-ESM	GCESS/BNU	26	2.194 hPa	Low
CanESM2	CCC	35	0.5 hPa	Mid
CCSM4	NCAR	27	2.194 hPa	Low
CMCC-CESM	CMCC	39	0.01 hPa	High
CMCC-CM	CMCC	31	10 hPa	Low
CMCC-CMS	CMCC	95	0.01 hPa	High
CNRM-CM5	CNRM	31	10 hPa	Low
CSIRO-Mk3-6-0	CSIRO/QCCCE	18	4.5 hPa	Low
FGOALS-g2	LASG/IAP	26	2.194 hPa	Low
GFDL-CM3	GFDL	48	0.01 hPa	High
GFDL-ESM2G	GFDL	24	3 hPa	Low
GFDL-ESM2M	GFDL	24	3 hPa	Low
HadGEM2-CC	MOHC	60	84 km	High
INMCM4	INM	21	10 hPa	Low
IPSL-CM5A-LR	IPSL	39	0.04 hPa	High
IPSL-CM5A-MR	IPSL	39	0.04 hPa	High
IPSL-CM5B-LR	IPSL	39	0.04 hPa	High
MIROC5	AORI/NIES/JAMSTEC	40	3 hPa	Low
MIROC-ESM	AORI/NIES/JAMSTEC	80	0.0036 hPa	High
MIROC-ESM-CHEM	AORI/NIES/JAMSTEC	80	0.0036 hPa	High
MPI-ESM-LR	MPI	47	0.01 hPa	High
MPI-ESM-MR	MPI	95	0.01 hPa	High
MRI-CGCM3	MRI	48	0.01 hPa	High
NorESM1-M	NCC	26	3.54 hPa	Low

Table 2 Sudden stratospheric warming (SSW) identified from the wind reversal and wind tendency definitions.

Number	Central dates at 60°N	
	reversal	tendency
1	31 Jan 1958	30 Jan 1958
2	17 Jan 1960	18 Jan 1960
3	28 Jan 1963	27 Jan 1963
4	16 Dec 1965	
5	23 Feb 1966	27 Feb 1966
6	7 Jan 1968	2 Jan 1968
7	28 Nov 1968	
8	13 Mar 1969	
9	2 Jan 1970	6 Jan 1970
10	18 Jan 1971	15 Jan 1971
11	20 Mar 1971	
12		28 Feb 1972
13	31 Jan 1973	1 Feb 1973
14		28 Feb 1974
15	9 Jan 1977	
16		2 Feb 1978
17		27 Jan 1979
18	22 Feb 1979	27 Feb 1979
19	29 Feb 1980	
20		31 Jan 1981
21	4 Mar 1981	
22	4 Dec 1981	
23		31 Jan 1983
24	24 Feb 1984	19 Feb 1984
25	1 Jan 1985	3 Jan 1985
26	23 Jan 1987	24 Jan 1987
27	8 Dec 1987	10 Dec 1987
28	14 Mar 1988	
29	21 Feb 1989	11 Feb 1989
30		15 Feb 1990
31		4 Feb 1991
32		16 Jan 1992
33		18 Feb 1993
34		27 Jan 1995
35	15 Dec 1998	19 Dec 1998
36	26 Feb 1999	28 Feb 1999
37	20 Mar 2000	
38	11 Feb 2001	9 Feb 2001
39	31 Dec 2001	2 Jan 2002
40	18 Feb 2002	

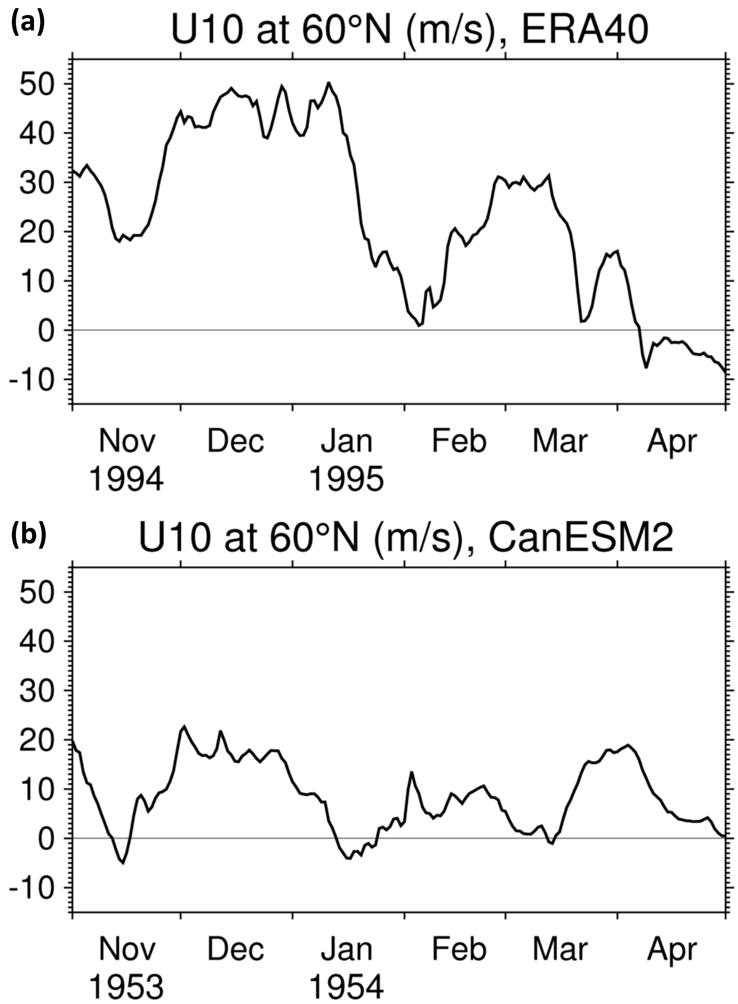

Fig. 1 Zonal-mean zonal winds (m s^{-1}) at 10 hPa and 60°N for (a) ERA40 and (b) CanESM2 models. The thin line across the x-axis denotes the 0 m s^{-1} threshold.

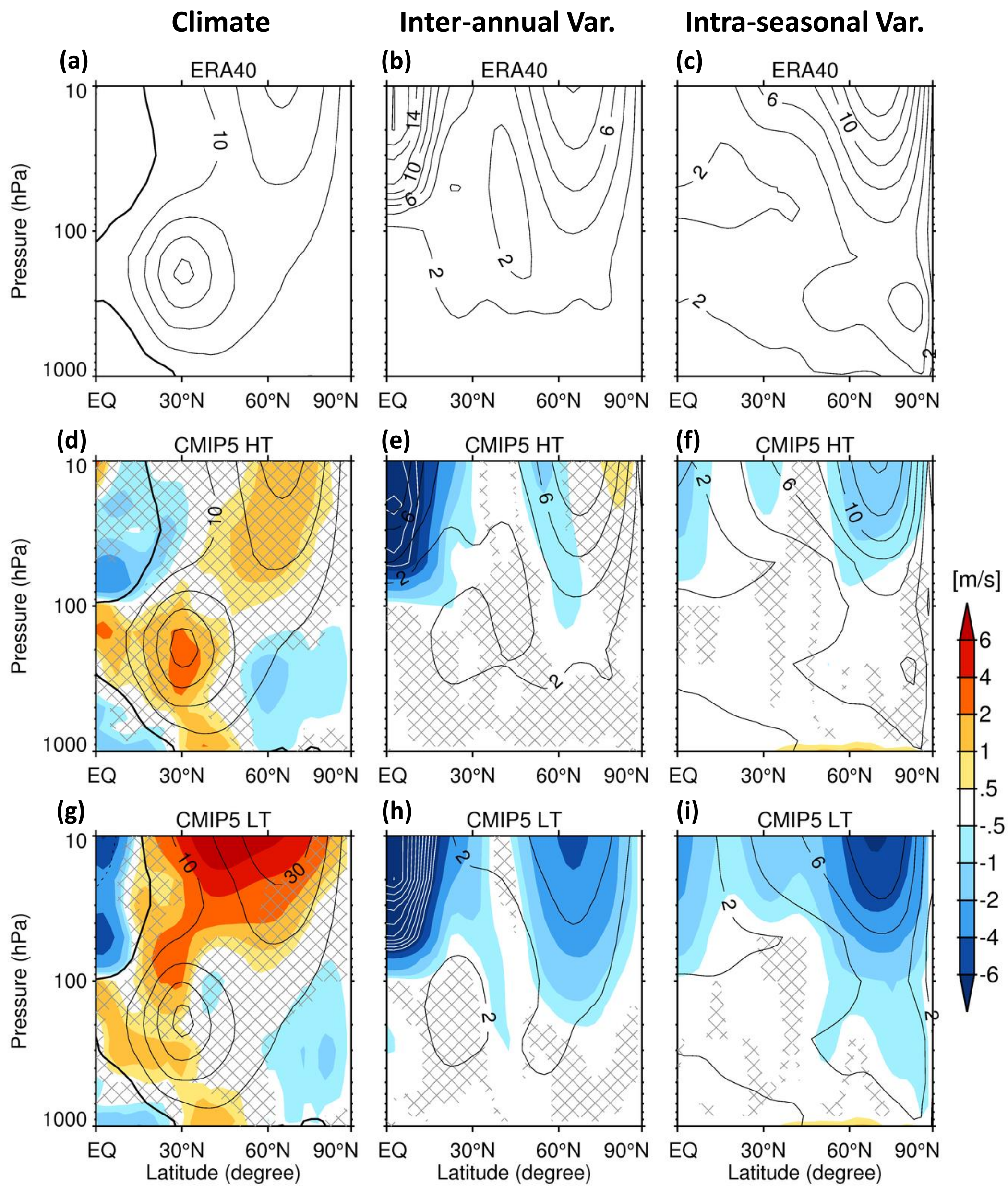

Fig. 2 (a) Latitude and height cross-section of the climatological zonal-mean zonal winds ([u]; m s^{-1}) averaged from December to February (DJF) in ERA40. The contour interval is 10 m s^{-1}, and the zero line is indicated with a thick black line. (center and right) Same as (a) but for interannual variability of the DJF-mean [u] (center) and daily variability of [u] in DJF (right). For the daily variability, the mean value for each winter was subtracted from daily anomalies to remove the impact of the interannual variability. (middle and bottom rows) Same as the top row but for high-top (middle) and low-top (bottom) models. Statistically insignificant (t-test; $p > 0.05$) values are hatched, and difference from ERA40 (model-ERA40) is shown by shading.

683

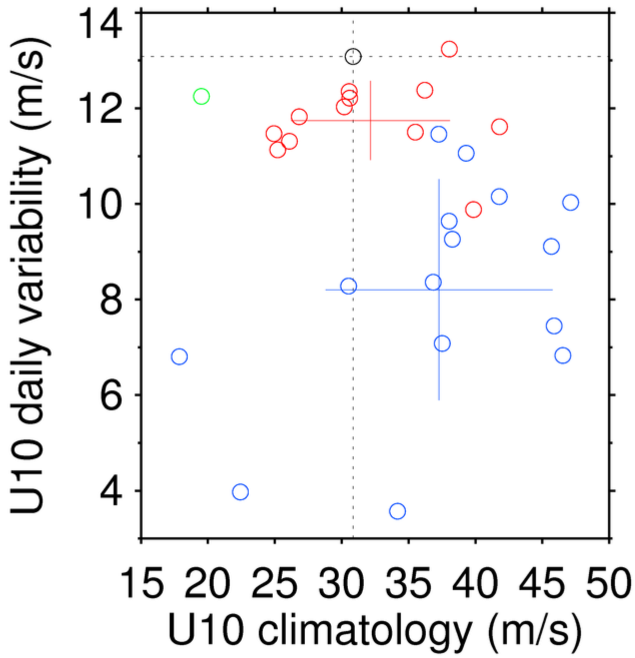

Fig. 3 Scatter plot of the zonal-mean zonal wind climatology at 10 hPa and at 60°N and its daily standard deviation from CMIP5 models. Red, green, blue, and black colors indicate high-top, mid-top, and low-top models and ERA40 reanalysis, respectively. Solid lines range ±1 standard deviation among models while centered on their multi-model mean.

684

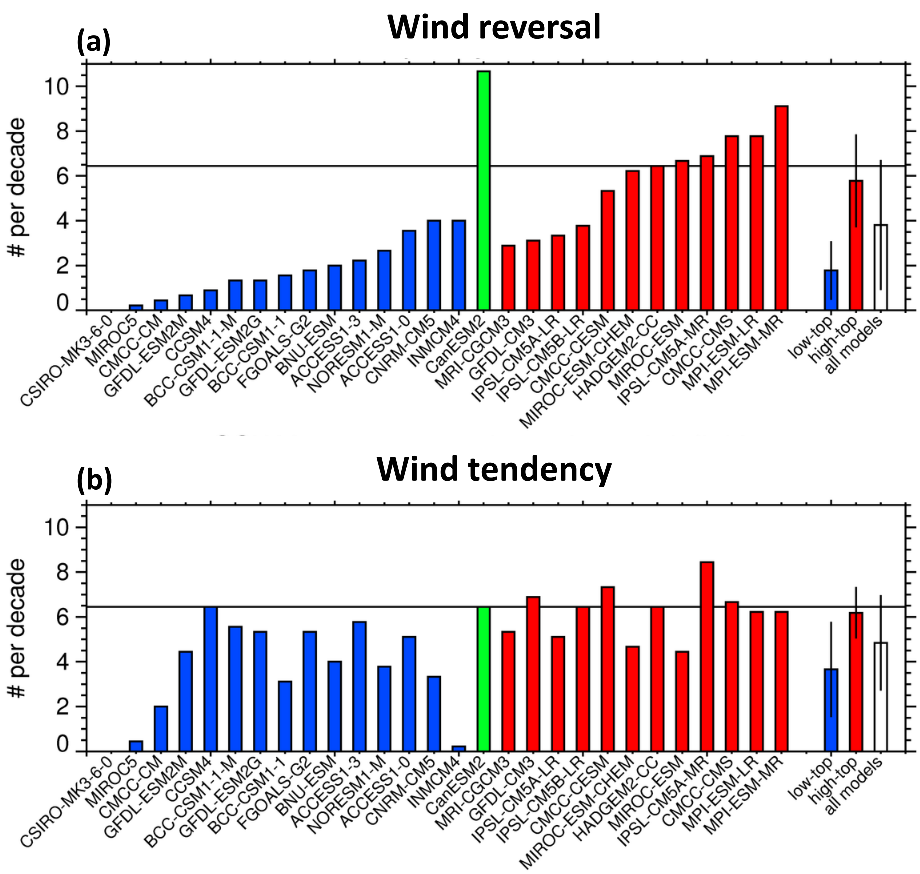

Fig. 4 Sudden stratospheric warming (SSW) frequency derived from (a) the wind reversal definition and (b) the wind tendency definition. Low-top, mid-top, and high-top models are colored blue, green, and red, respectively. The SSW frequency in ERA40 is indicated by the black horizontal line. Multi-model mean frequency and intermodel spread (1 standard deviation) are shown at the right of each panel.

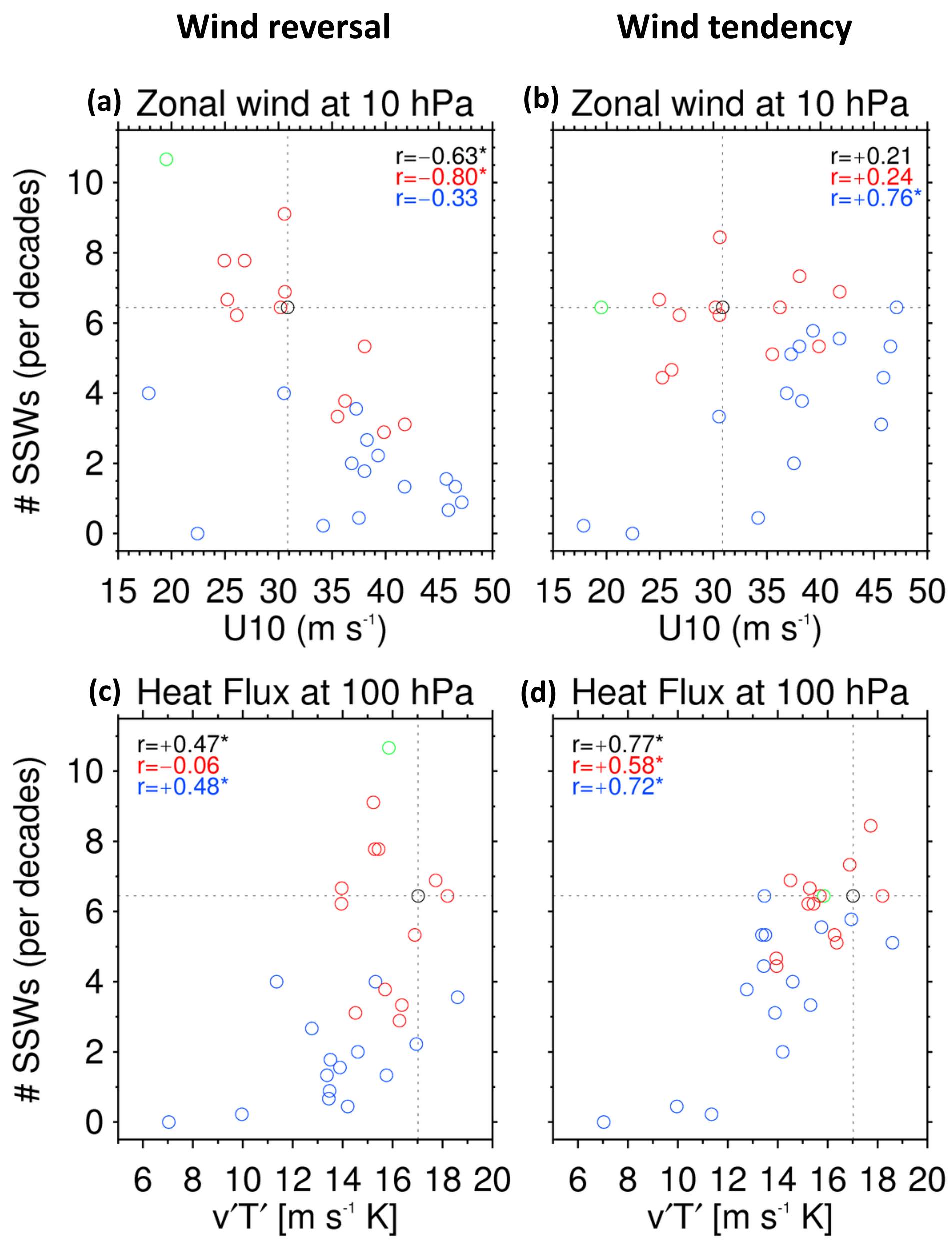

Fig. 5 (a, b) Scatter plot of climatological zonal-mean zonal wind at 10 hPa and 60°N and sudden stratospheric warming (SSW) frequency for the wind reversal definition (left) and the wind tendency definition (right). (c, d) Same as top panels but for eddy heat flux at 100 hPa integrated over 45–75°N. Low-top, mid-top, and high-top models are colored blue, green, and red, respectively. Black-dotted lines indicate the reference values in ERA40. The numbers shown in each panel denote the correlation coefficients for all (black), high-top (red), and low-top (blue) models. Statistically significant correlation coefficient at the 95% confidence level is indicated by the asterisk.

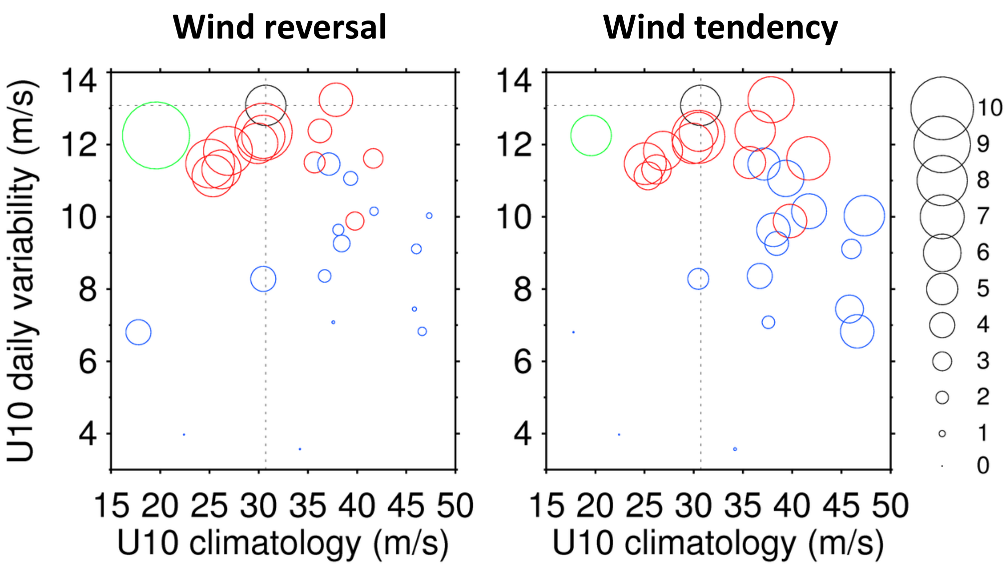

Fig. 6 Same as Fig. 3 but for sudden stratospheric warming (SSW) frequency introduced using the wind reversal definition (left) and the wind tendency definition (right). The circle size indicates the SSW frequency per decade. Low-top, mid-top, and high-top models are colored blue, green, and red, respectively.

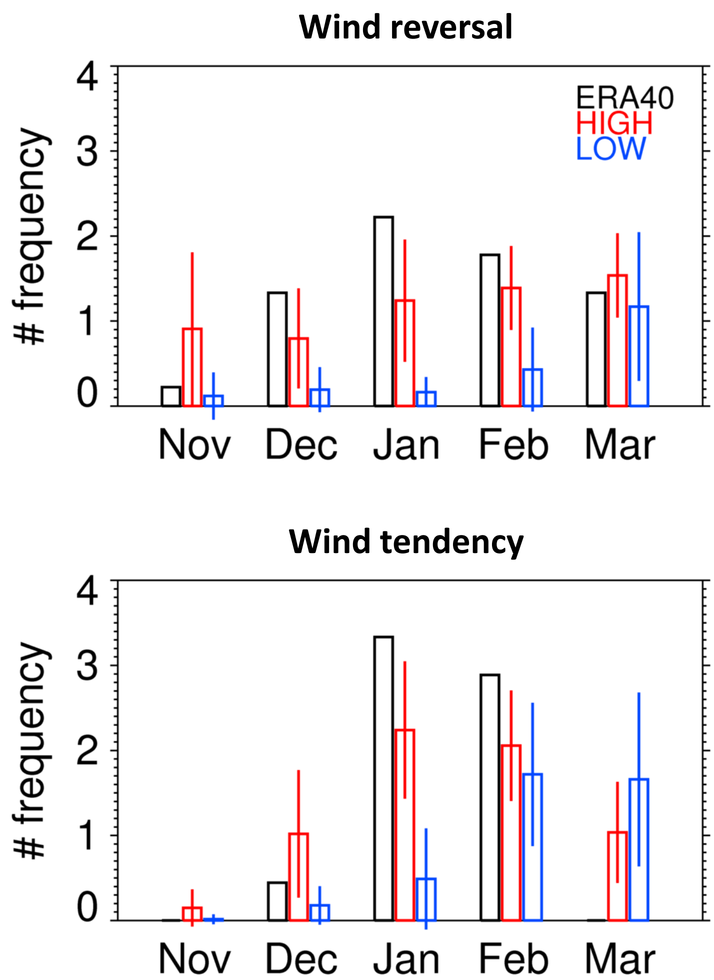

Fig. 7 Distribution of stratospheric warmings by month in ERA40 reanalysis (black), high-top (red), and low-top models (red) derived from (top) the wind reversal definition and (bottom) the wind tendency definition. Vertical lines at high-top and low-top models indicate the ±1 standard deviation of SSW frequency from the mean of each model.

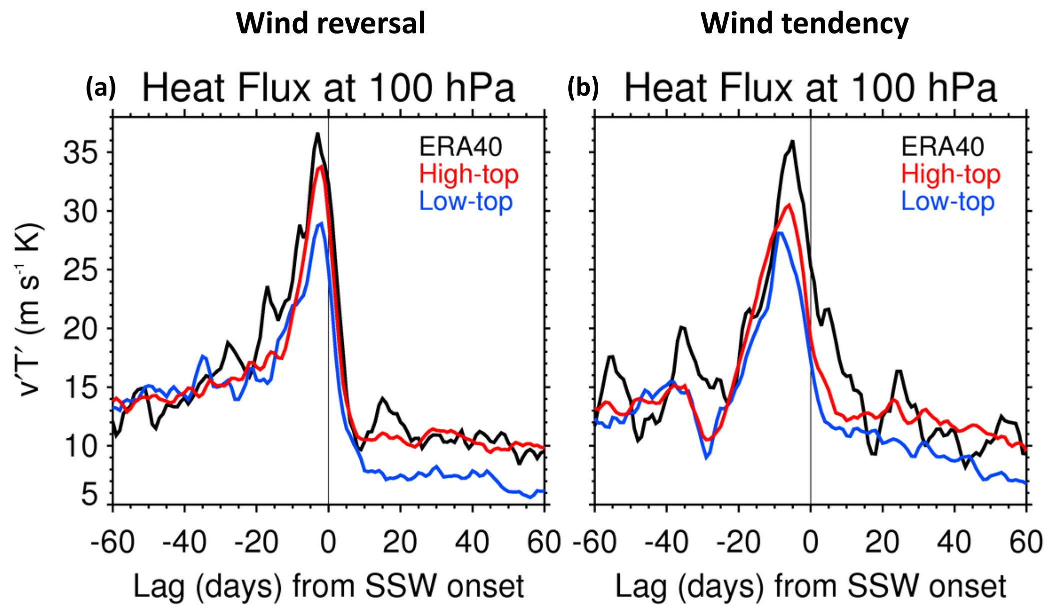

Fig. 8 Multi-model mean time series of zonal-mean eddy heat flux at 100 hPa integrated over 45–75°N during sudden stratospheric warming (SSW) detected by the wind reversal definition (left) and the wind tendency definition (right). Lag zero indicates the onset of SSW. Low-top and high-top models are denoted by blue and red colors, respectively. The reference time series, derived from ERA40, is shown in black.

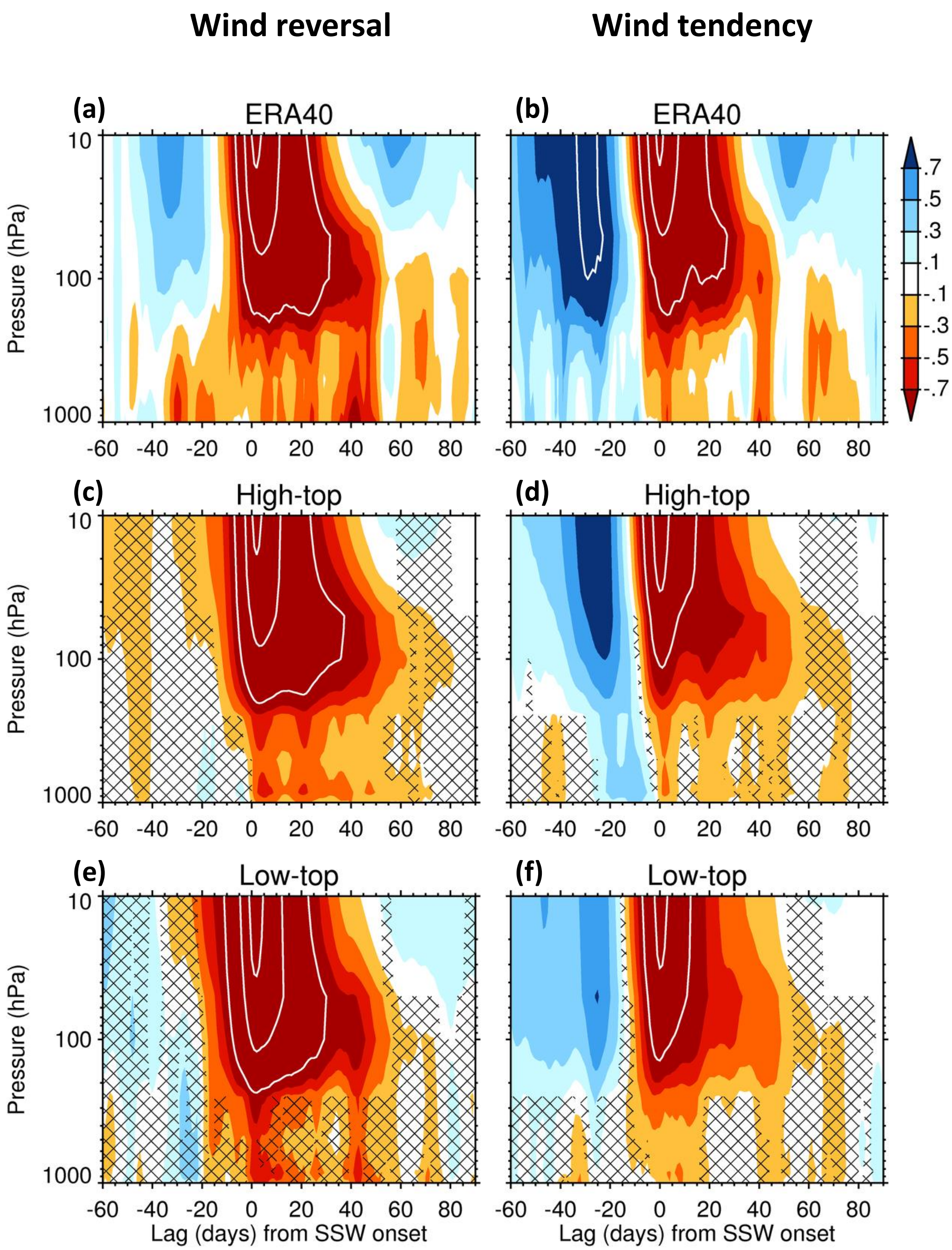

Fig. 9 Time-height development of the northern annular mode (NAM) index during sudden stratospheric warming (SSW) events, as detected by the wind reversal definition (left) and the wind tendency definition (right) for ERA40 (top), high-top (middle), and low-top (bottom) models. The NAM index is based on polar-cap averaged geopotential height (>60°N). Shading interval of 1.0 is indicated by a white line. Hatching shows insignificant values (95%) when the multi-model spread is considered.

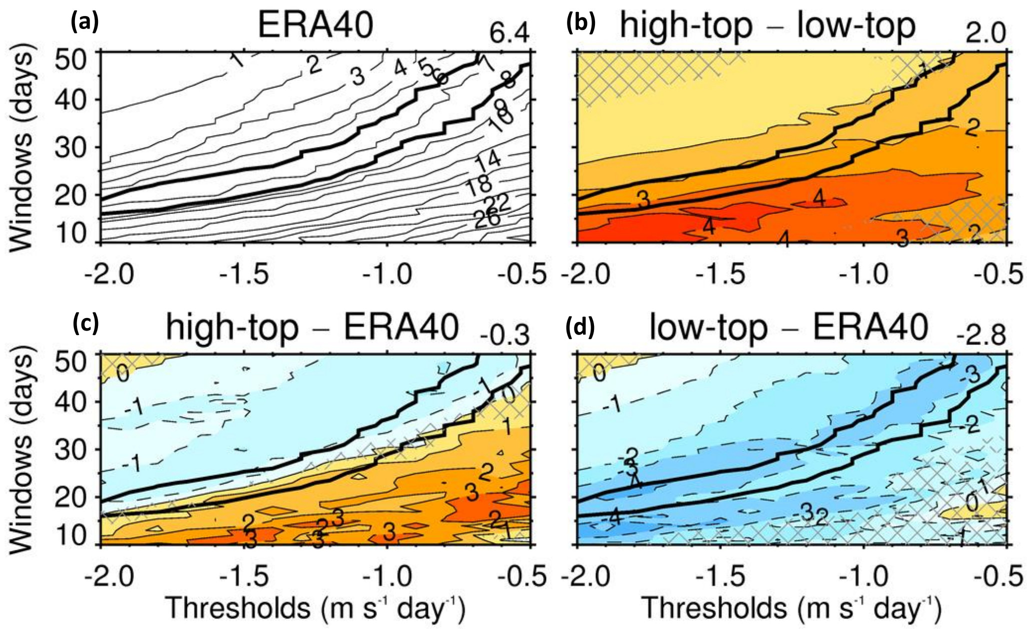

Fig. 10 (a) Sudden stratospheric warming (SSW) frequency as a function of the threshold value of the zonal-mean zonal wind tendency at 10 hPa and 60°N and the evaluated time window for ERA40. (b) Difference between the high-top and low-top models. Difference between ERA40 and (c) high-top and (d) low-top models. Values statistically insignificant at the 95% confidence level are hatched. The two low-top models were ignored because their SSWs are extremely rare. The SSW frequency of six to eight events per decade from ERA40 is shown by with thick black lines in each panel. The numbers at the upper right corner in each panel indicates SSW frequency or its difference from ERA40 when the -1.1 m s^{-1} day^{-1} threshold and 30-day time window are used.

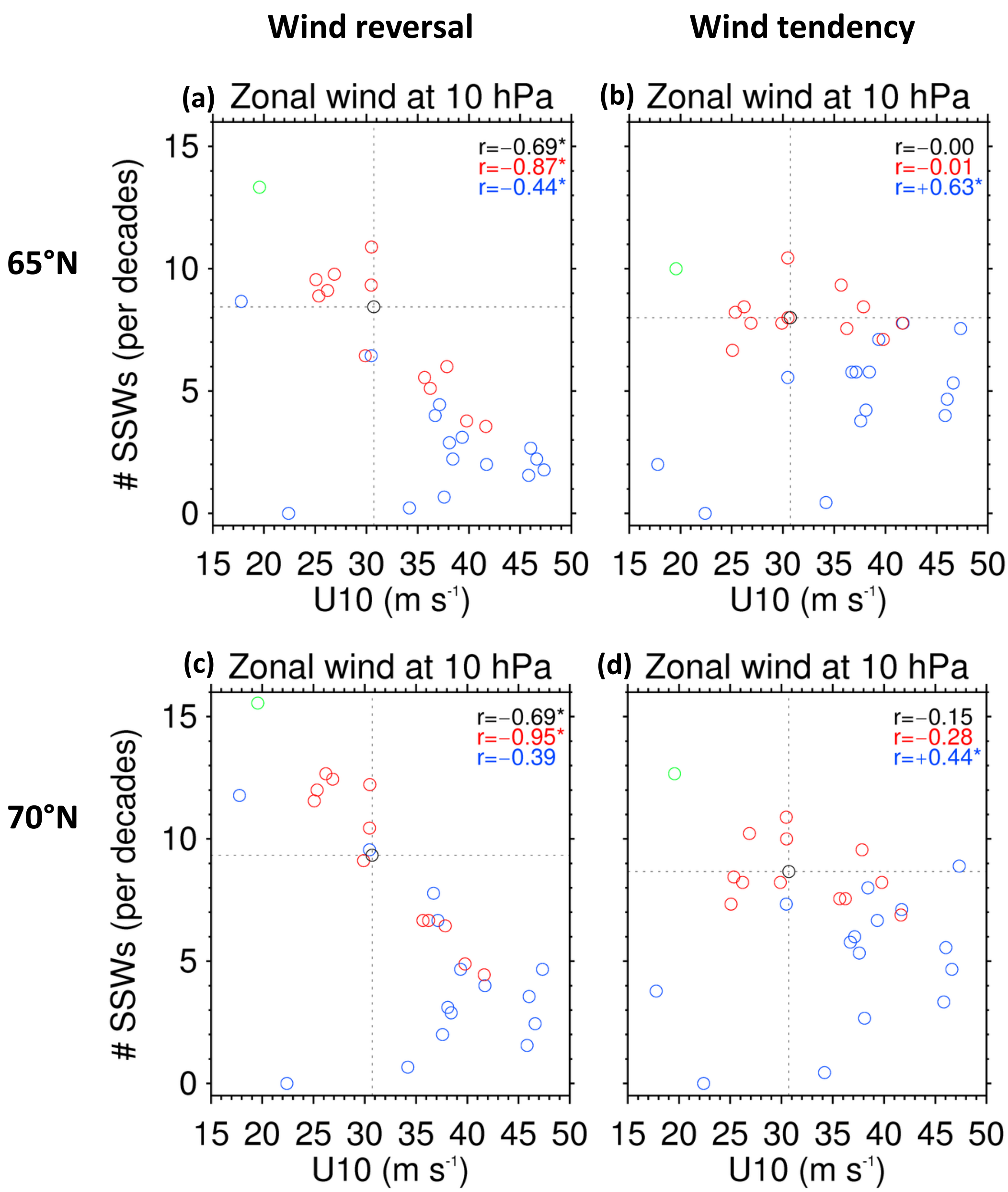

Fig. 11 (a, b) Scatter plot of climatological zonal-mean zonal wind at 10 hPa and 65°N, and SSW frequency for (left) the wind reversal definition and (right) the wind tendency definition. (c, d) Same as top panels but for zonal wind at 70°N. Low-top, mid-top, and high-top models are colored with blue, green, and red, respectively. Black-dotted lines indicate the reference values in ERA40. Numbers shown in each panel denote the correlation coefficients for (black) all, (red) high-top, and (blue) low-top models. Statistically significant correlation coefficient at the 95% confidence level is indicated by asterisk.

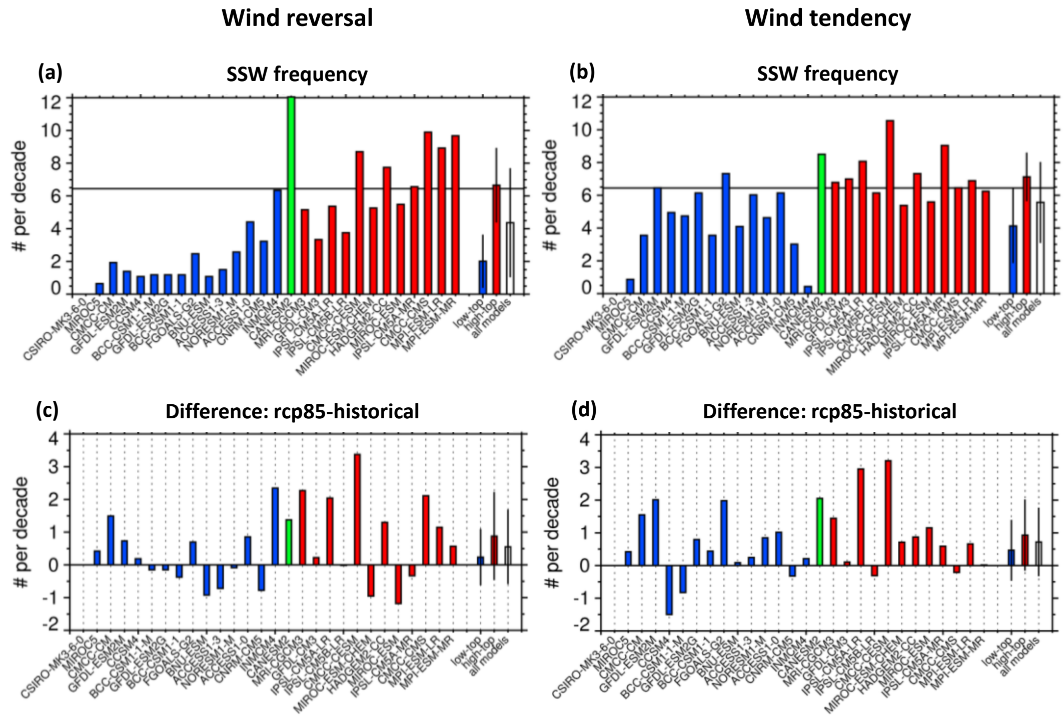

Fig. 12 (a, b) Same as Fig. 4 but for RCP8.5 runs. (c, d) Difference in sudden stratospheric warming (SSW) frequency between RCP8.5 and historical runs.